Initial results from 3-D MHD simulation studies for low-A RFP

Akio Sanpei, Sadao Masamune and RELAX group
Kyoto Institute of Technology, Japan

Naoki Mizuguchi
National Institute of Fusion Science, Japan

Lower *A* has a possibility to easy access to QSH

Dependence of q-profile on A

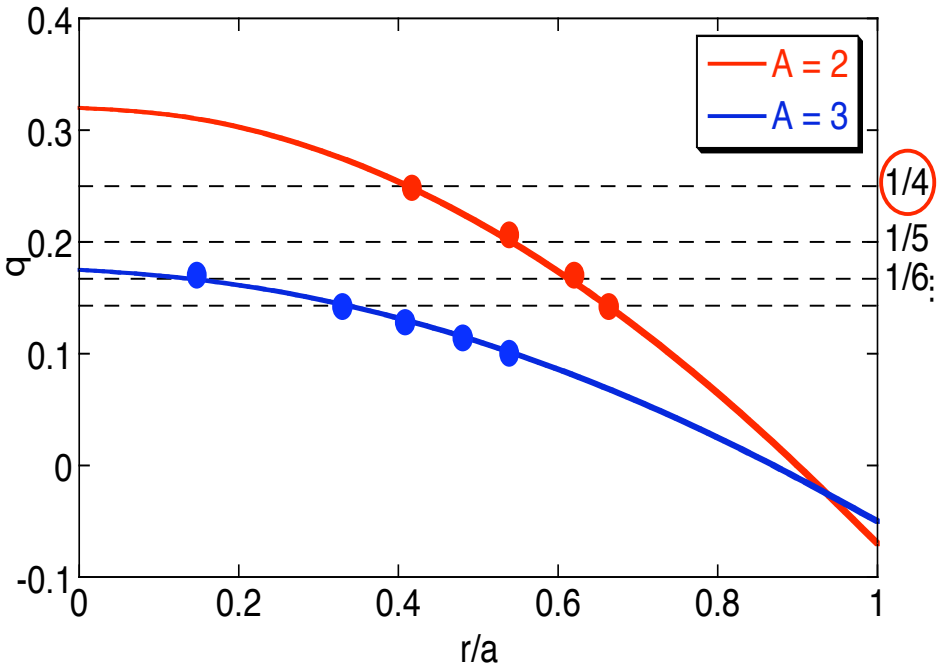

Lowering A leads to …

***q* in the core region : Up ↑**

m=1 modes resonant surfaces are less densely spaced in the core region.

Avoidance of overlap of magnetic islands (chaos).

expected

- **A simpler magnetic mode dynamics**
- **Easier access to the QSH RFP state**

REversed field pinch of Low-Aspect-ratio eXperiment

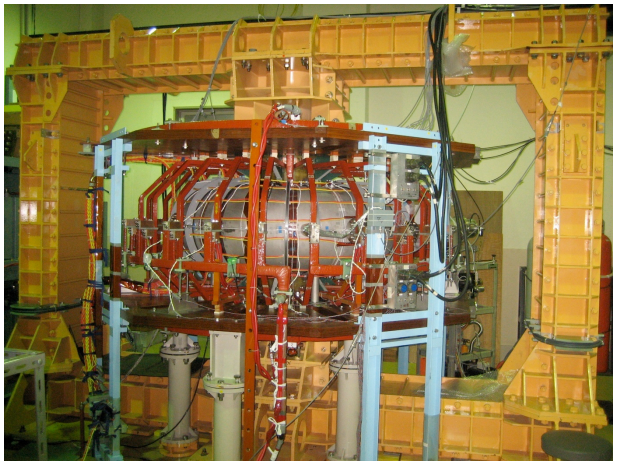

Vacuum vessel: SS (4mm t)

R : 0.51 m

a : 0.25 m

A : 2

Toroidal field : ~0.1T

Plasma current : ~100kA

Examples of RELAX discharge

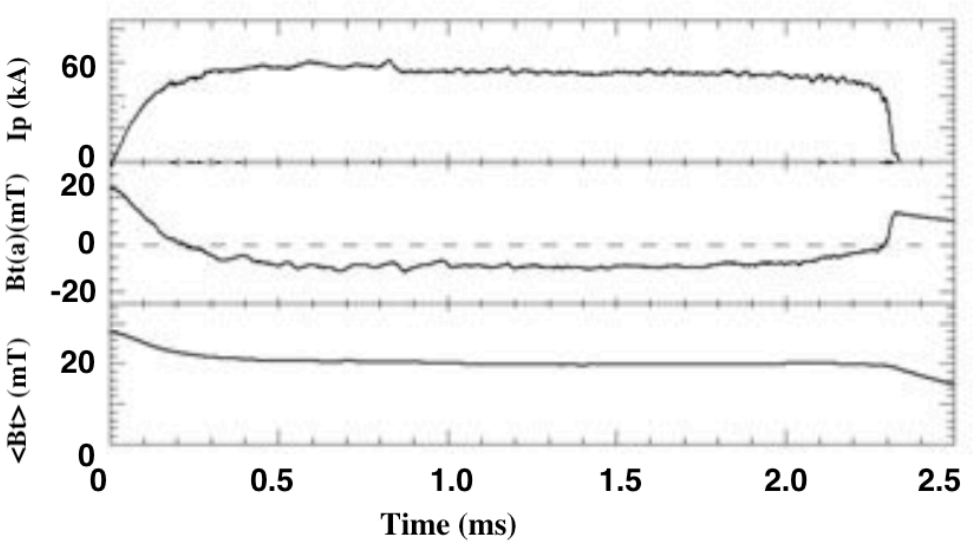

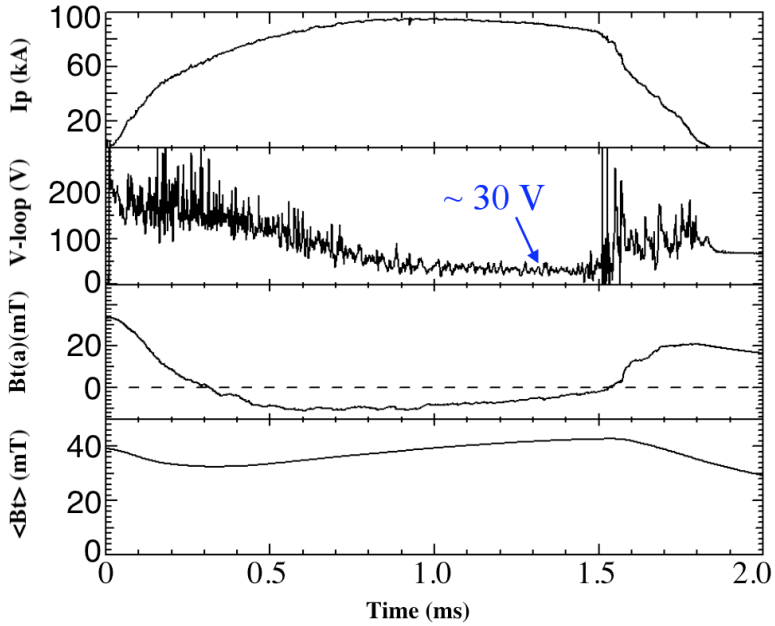

Operation regimes in (Theta, F) space in RELAX

$$F \equiv \frac{B_\phi(a)}{\langle B_\phi \rangle}$$

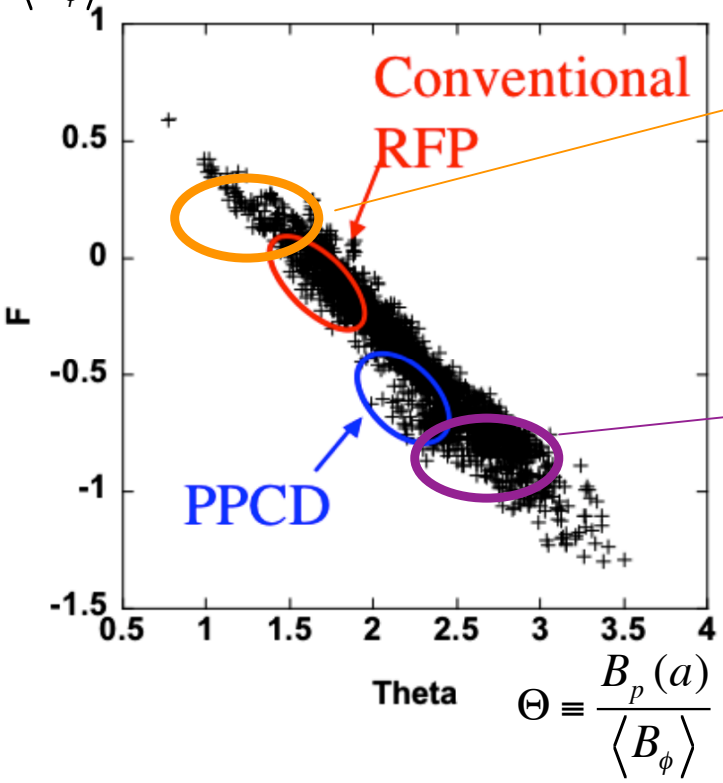

$$\Theta \equiv \frac{B_p(a)}{\langle B_\phi \rangle}$$

Discharge regime in F-Θ space extended to higher Θ, deeper F without any disruption in low-A RFP.

The toroidal mode spectrum of edge magnetic fluctuations, and q-profile

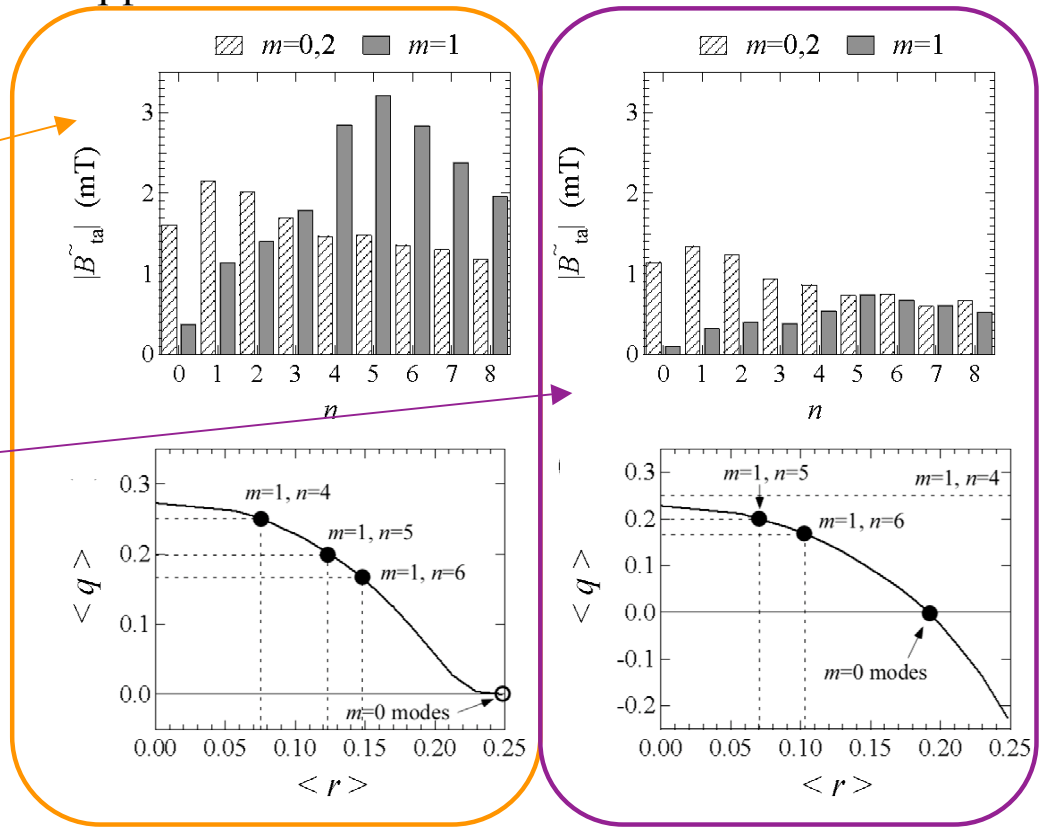

The toroidal mode spectrum is narrowed by reducing the toroidal field reversal, and the QSH state tends to be realized in shallow reversal discharges.

Magnetic measurement suggests Helical structure in shallow reversal in RELAX

Radial arrays of magnetic probes
inserted from outward-port
into the plasma region

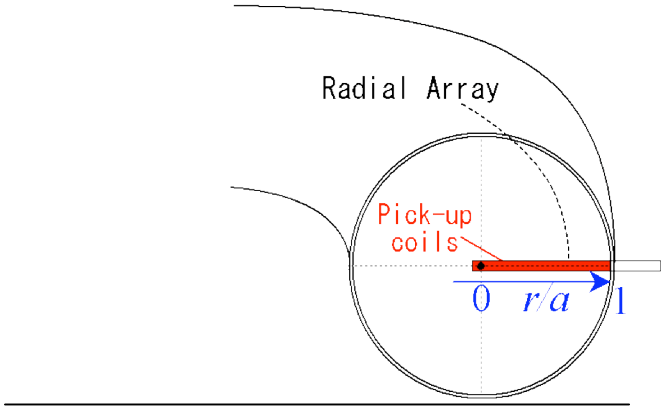

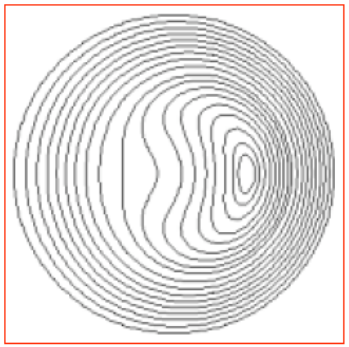

Contours of helical flux function in HOE

Comparison of profile of measurement with each component in HOE.

Non-oscillating component

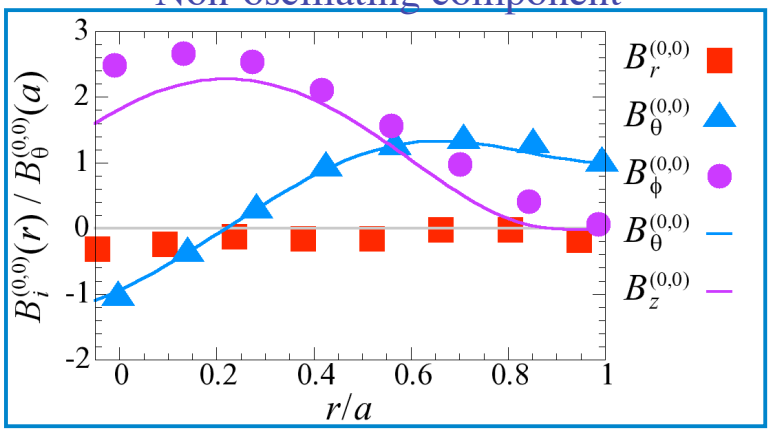

oscillating component

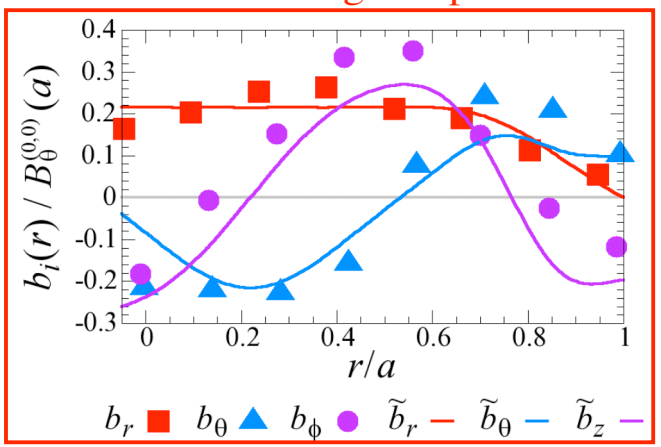

HOE is realized in RELAX.

SXR imaging measurement also suggests helical structure in shallow reversal in RELAX

SXR imaging measurement

In order to study the plasma structure in very shallow reversal region, we have taken SXR tangential images using a SXR pin-hole camera.

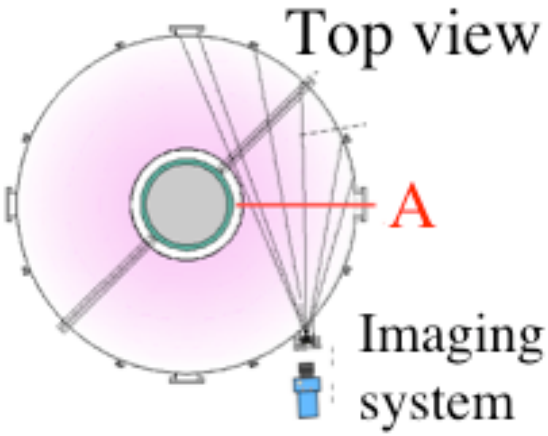

An experimental SXR image with 5-micro sec exposure during a single m=1/n=4 mode dominated period.

Obtained image

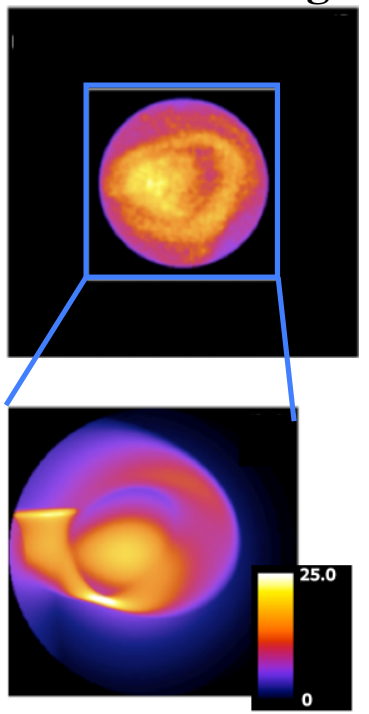

Calculated image

The helix similar to the experimental result was reproduced in the calculated image.

The results have shown that there exist core region with simple helical structure.

3-D MHD simulation

We are interested in theoretical formation of such helical deformation in fully toroidal system.

Direct numerical simulations of the fully three-dimensional, nonlinear MHD equations in a low-A RFP plasma.

(1979) Sato and Hayashi for Spheromac
(2000) Hayashi and Mizuguchi for ST

This simulation code successfully reproduces several key features of Internal Reconnection Event in spherical tokamak.

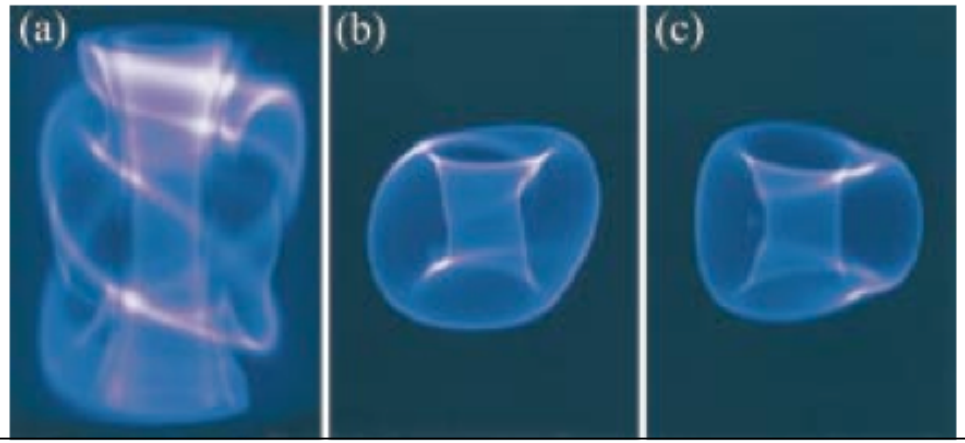

Mizuguchi et al., Phys. Plasmas, Vol. 7, 940 (2000)

(Now) Mizuguchi and RELAX group for RFP

Set up of 3-D MHD simulation on A=2 RFP

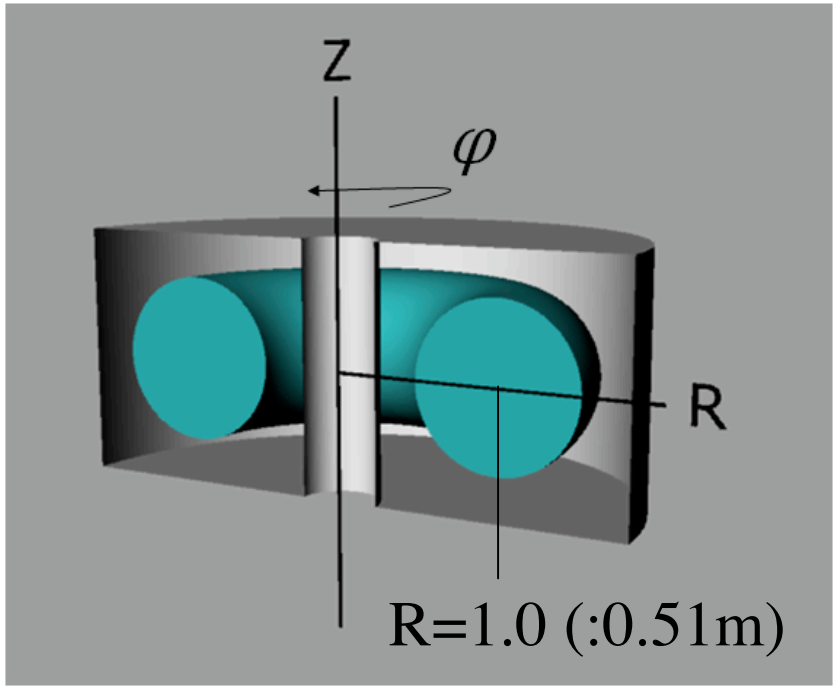

We concentrate our interest on Toroidal effect.

Boundary condition

The boundary condition is put as a perfect-conducting and no-slip wall at all boundaries of the computation region.

- $\mathbf{B}_{\perp}$=const. $\mathbf{V}$=0, $\mathbf{j}$=0 at the boundary
- meshes: $(N_R \times N_\phi \times N_Z) = (153 \times 128 \times 153)$

Initial plasma region

$0.5 < R < 1.5$

$0 < \phi < 2\pi$

$-0.5 < Z < 0.5$

Calculation region

$0.240 < R < 1.76$

$0 < \phi < 2\pi$

$-0.760 < Z < 0.760$

The framework of the simulation code is a finite-difference and an explicit time-integration scheme.

Set up of 3-D MHD simulation on A=2 RFP

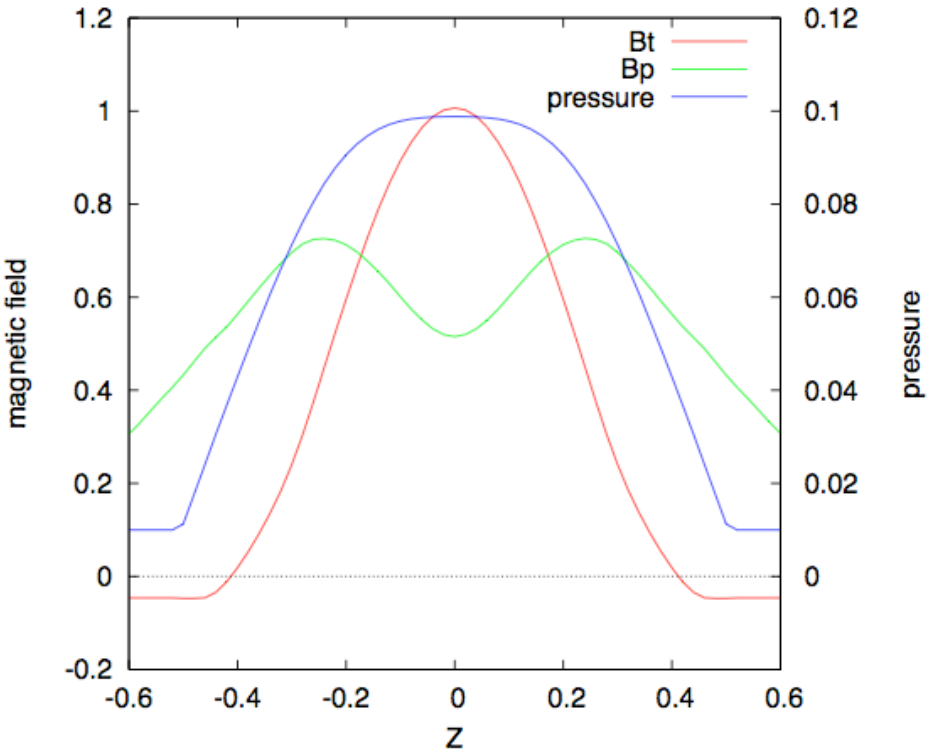

Initial distribution

Reconstructed equilibrium from experimental result of RELAX with Fit code.

(torus symmetric)

η :resistivity

μ :viscosity

are uniform and constant on each case.

Perturbations

The simulation starts from a linearly unstable configuration which causes initial tiny perturbations to grow spontaneously. The perturbation is introduced on the plasma velocity field at t = 0 as a random white noise.

Visco-resistive MHD equations of the simulation

$$\frac{\partial \rho}{\partial t} = -\nabla \cdot (\rho \mathbf{V})$$

Equation of continuity

Fluid viscosity

$$\frac{\partial \rho \mathbf{V}}{\partial t} = -\nabla \cdot (\rho \mathbf{V}\mathbf{V}) + \mathbf{j} \times \mathbf{B} - \nabla p + \mu \left\{ \nabla^2 \mathbf{V} + \frac{1}{3} \nabla \left(\nabla \cdot \mathbf{V} \right) \right\}$$

Equation of motion

$$\mathsf{E} = -\mathsf{V} \times \mathsf{B} + \eta \mathsf{j}$$

Generalized Ohm's low

$$\mathsf{j} = \nabla \times \mathsf{B}$$

resistivity

$$\frac{\partial \mathbf{B}}{\partial t} = -\nabla \times \mathbf{E}$$

Maxwell equations

$$\frac{\partial p}{\partial t} = -\nabla \cdot (p\mathbf{V}) - (\gamma - 1)(p \nabla \cdot \mathbf{V} - \Phi - \eta \mathbf{j}^2)$$

Energy conservation

$$\Phi = 2\mu \left\{ e_{ij} e_{ij} - \frac{1}{3} \left(\nabla \cdot \mathbf{V} \right)^2 \right\}$$

$$e_{ij} = \frac{1}{3} \left(\frac{\partial V_i}{\partial x_j} + \frac{\partial V_j}{\partial x_i} \right)$$

Time is normalized with Alfven time.

Dependence on initial distribution

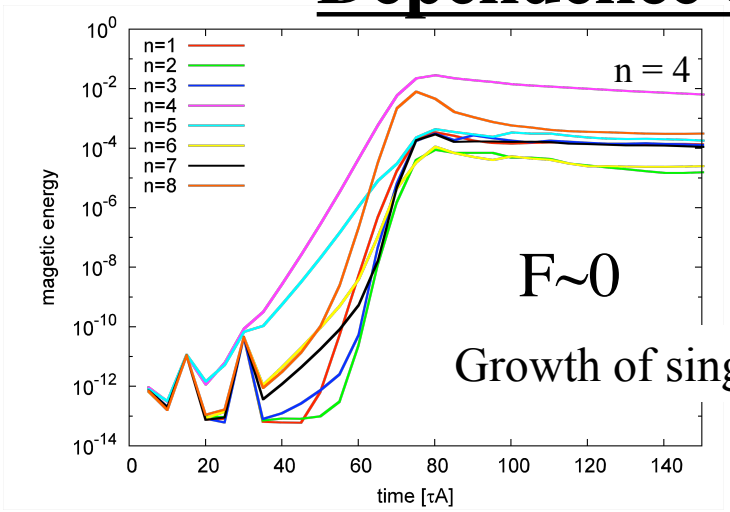

F~0

Growth of single mode

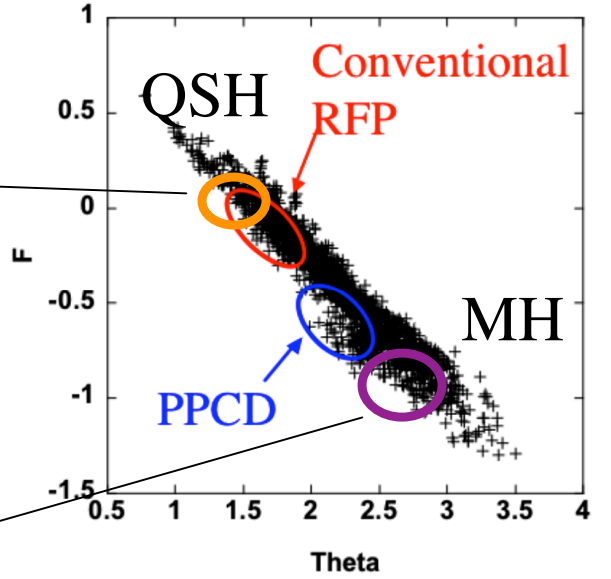

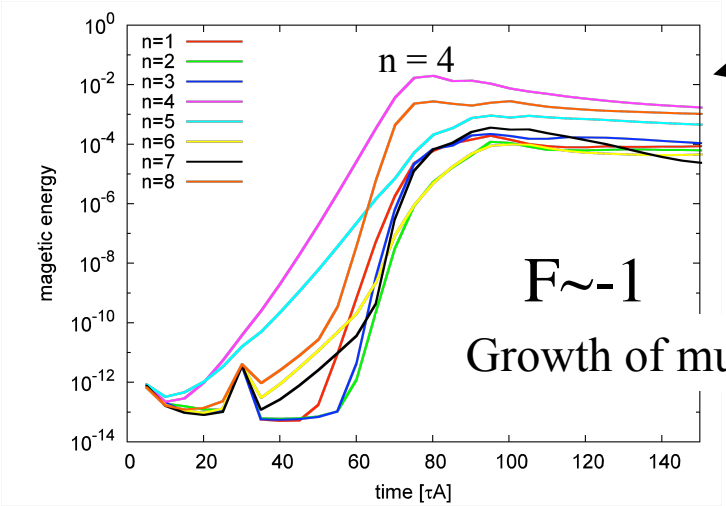

n = 8
n = 5

F~-1

Growth of multi mode

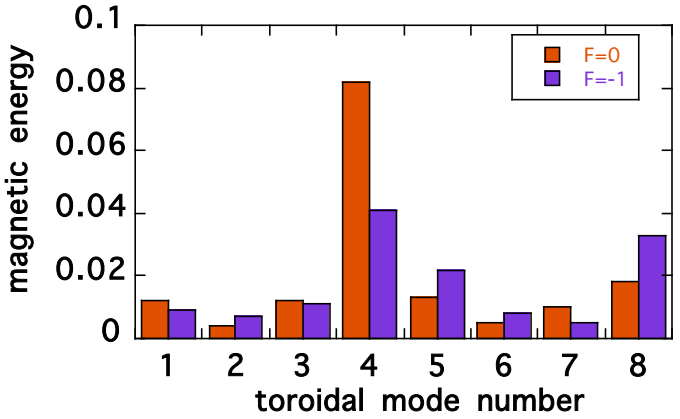

Mode spectrum at t=150

In the early stage of the growth until t~60, each of the components grows exponentially with its linear growth rate.

Dependence on initial distribution

Ratio of dominant mode to second mode at t=150.

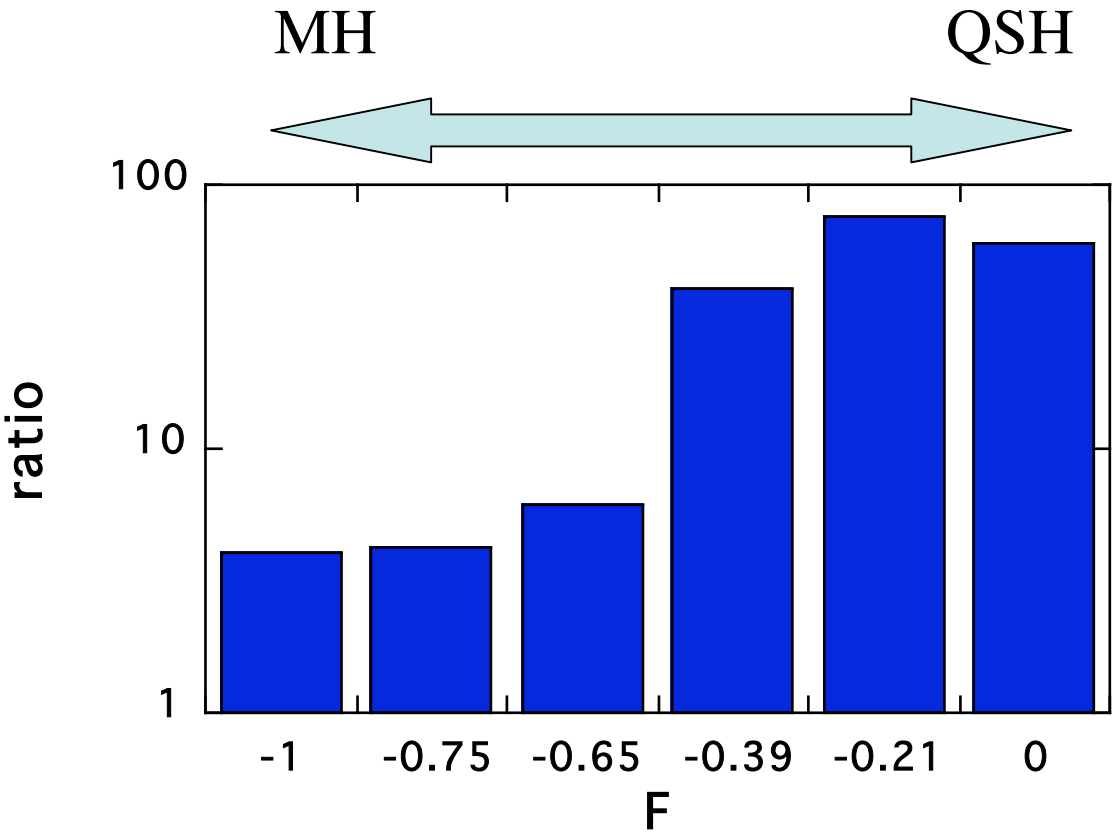

The ratio is suppressed by inducing the toroidal field reversal.

This tendency is consistent with experimental results.

Helical deformation of equi-pressure surface

(movie)

Equi-pressure surface

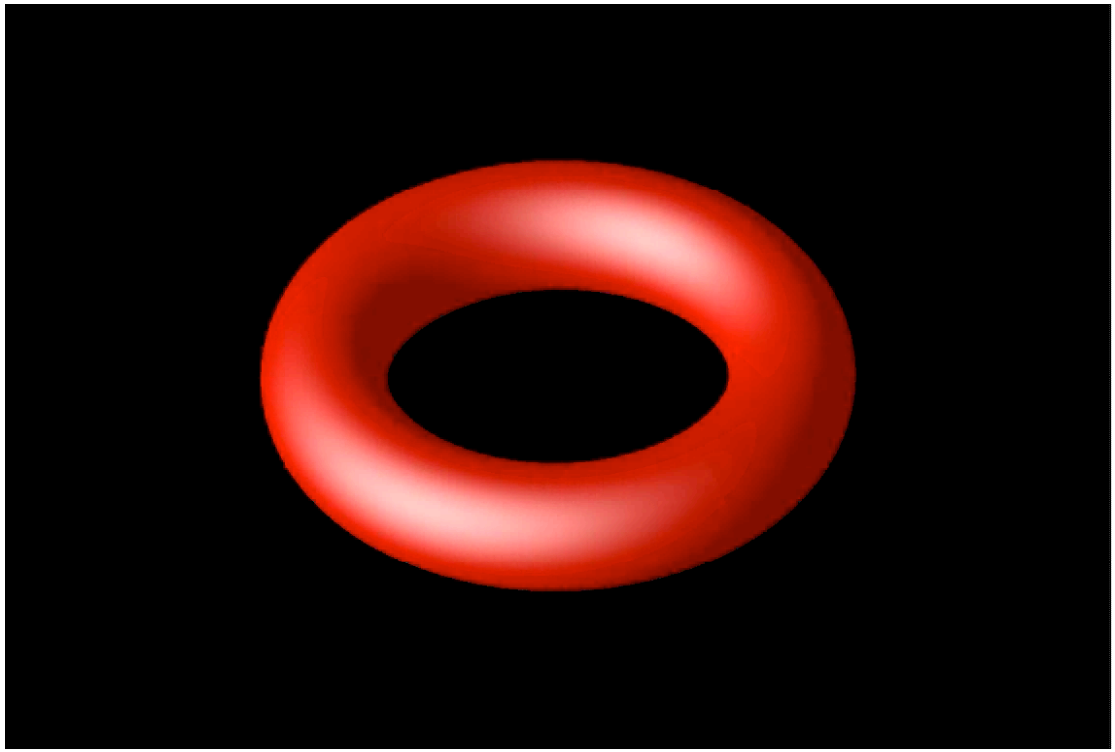

Pressure at center of poroidal cross-section

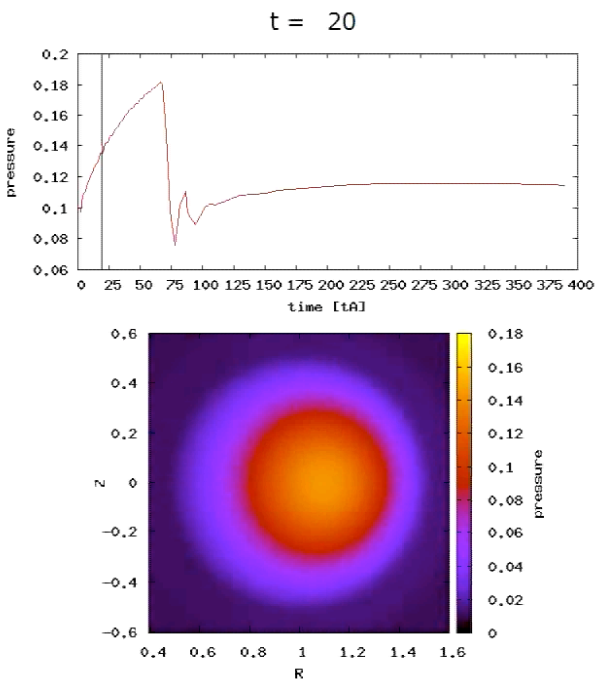

Pressure profile on poroidal cross-section

In the early stage of the growth until t=60, fluctuations grows exponentially.

In t~60, relaxation event occurs.

In the later stage, Helical deformation (m=1/n=4) remains.

Helical deformation of magnetic axis

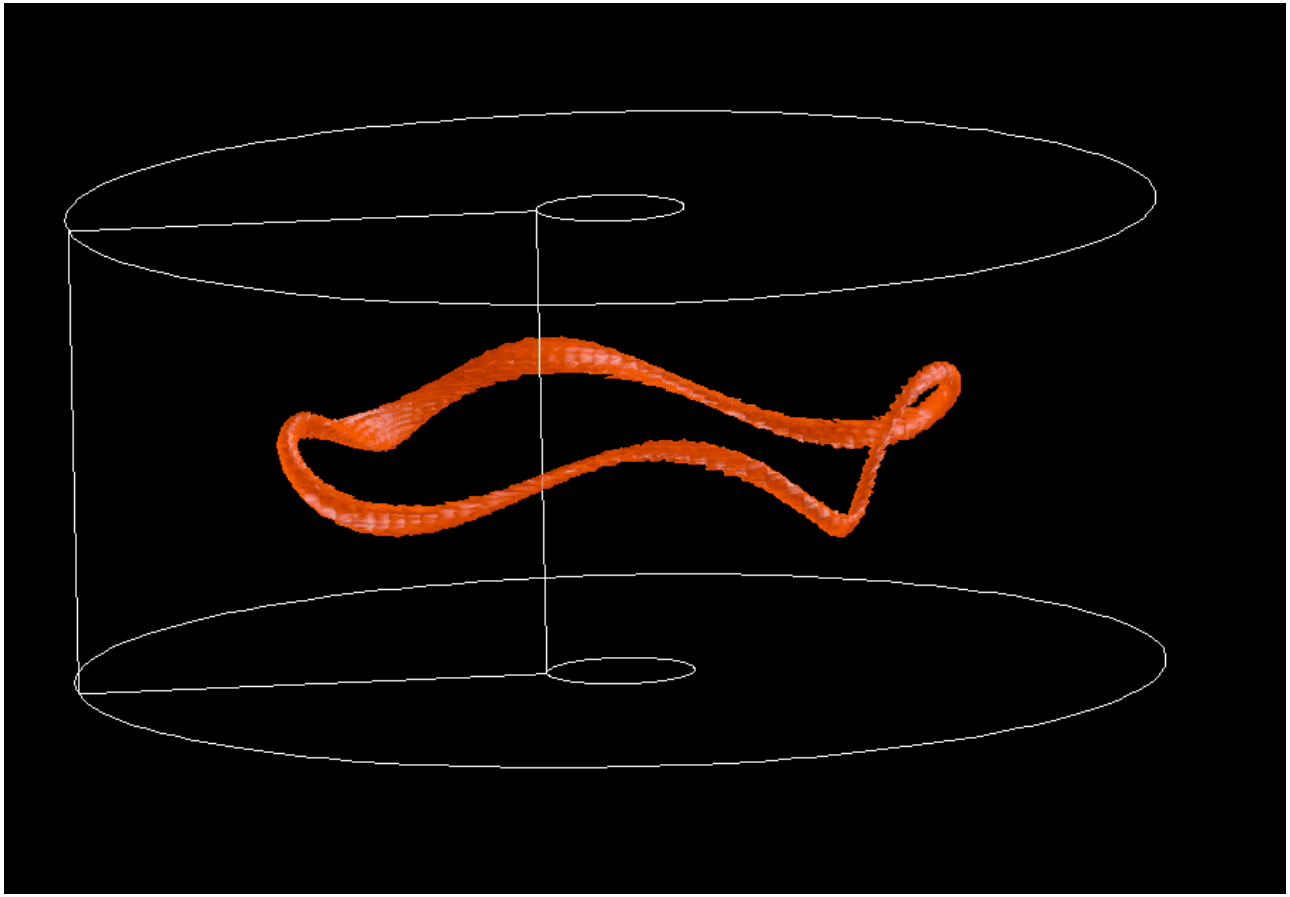

Magnetic axis deforms to helical structure at t=300.

In shallow-reversal discharge, formation of a self-organized m=1/n=4 structure is observed.

Helical deformation of equi-pressure surface

Snapshots of the pressure profile on poloidal cross-section.

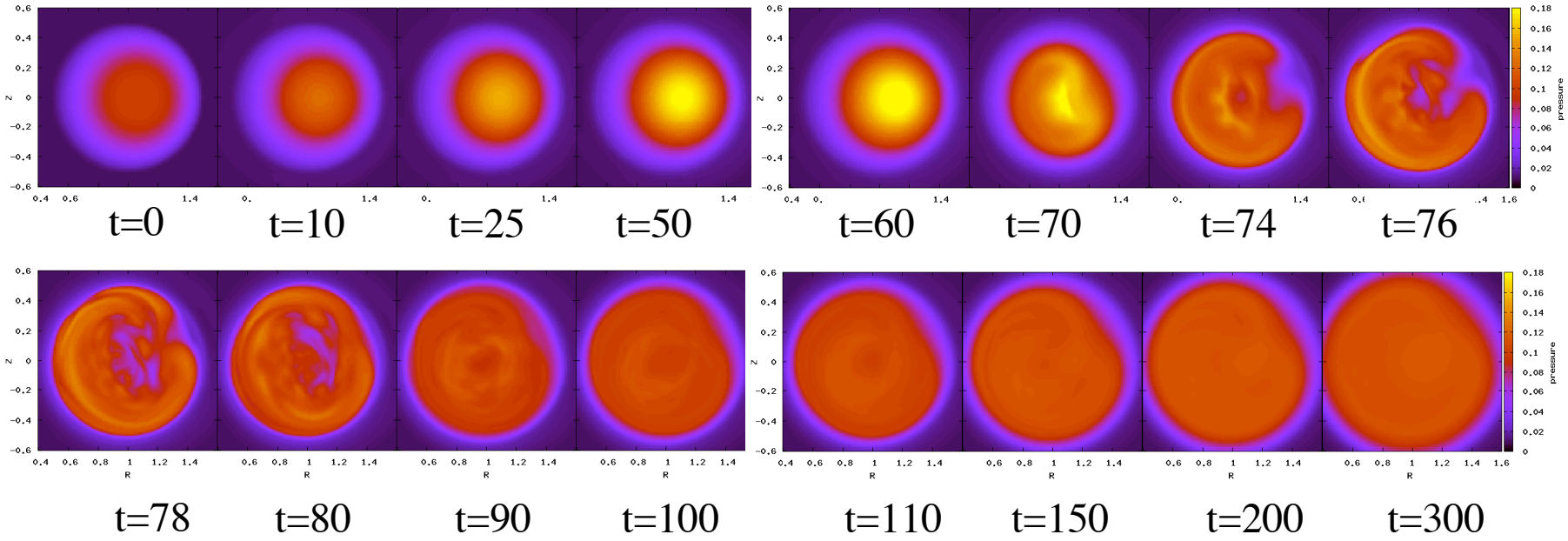

Pressure at center of poloidal cross-section increases due to joule heating.

The pressure profile is elliptically elongated in the poloidal cross section, reflecting the structure of m=1 mode.

The plasma pressure at the core region falls down by such relaxation in short time scale.

Pressure driven mode may be not dominant

To check a contribution of pressure driven instability, we carried out test simulation dropped the joule heating term from energy conservation

$$\frac{\partial p}{\partial t} = -\nabla \cdot (p\mathbf{V}) - (\gamma - 1)(p\nabla \cdot \mathbf{V} - \Phi - \eta \mathbf{j}^2)$$

included

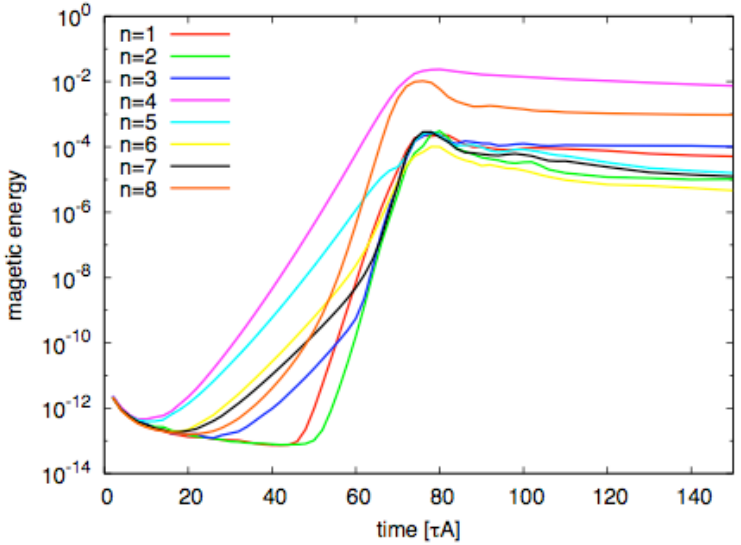

dropped

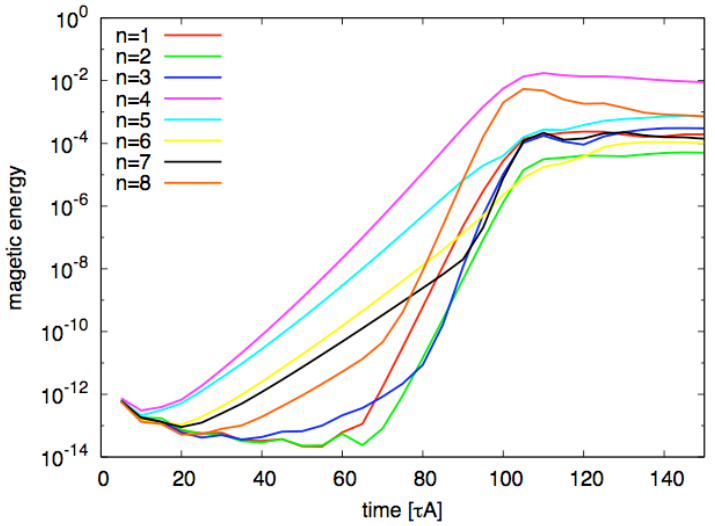

The growth rate for each toroidal mode number decreases.

Single m=1/n=4 mode growth is still observed.

Pressure driven instability exists, but it is not dominant.

Dependence of mode spectrum on Prandtl number

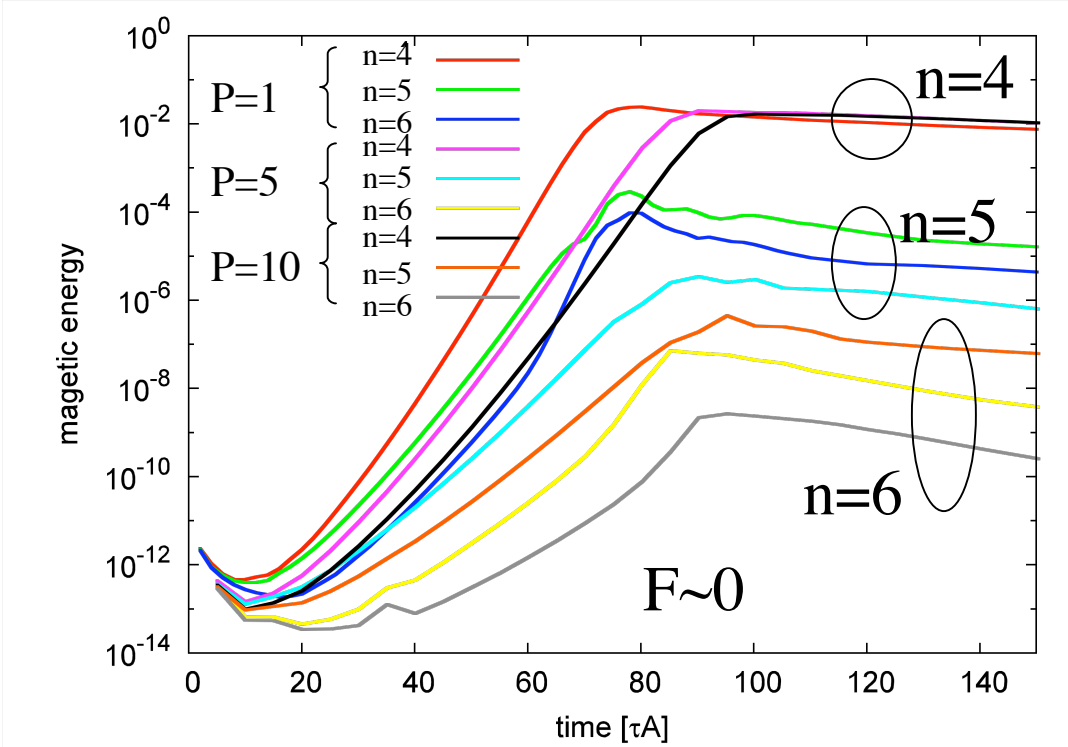

Prandtl number

$$P = \frac{\mu}{\eta}$$

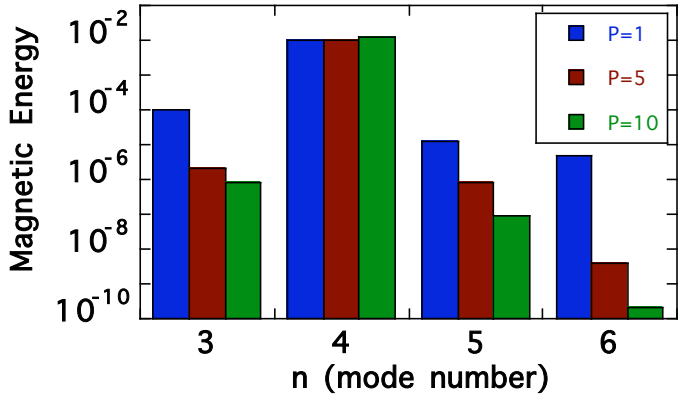

Mode spectrum at t=150

Growth of single mode (QSH) is observed.

Increasing of Plandtl number does not effective on dominant mode but reduce other mode.

The toroidal mode spectrum is narrowed by increasing the Plandtl number.

Summary

- Initial result of 3-D MHD simulation is demonstrated

  Dependence on initial distribution is consistent with experimental result.

  Helical deformation (m=1/n=4) is observed.

  The simulation has the possibility to explain the transition to m=1/n=4 deformation.

  The toroidal mode spectrum is narrowed by increasing the Plandtl number.

Future work

To continue parameter survey, about such as Hartmann number.

Change the boundary condition to circular.